

Received November 17, 2020; reviewed; accepted December 20, 2020

## Homogenization phenomena of surface components of fluorite and calcite

Ruofan Sun, Dan Liu, Benyue Zhang, Hao Lai, Shuming Wen

Faculty of Land Resource Engineering, Kunming University of Science and Technology, Kunming 650093, Yunnan, China  
State Key Laboratory of Complex Nonferrous Metal Resources Clean Utilization, Kunming 650093, Yunnan, China

Corresponding author: ldysyz1983@126.com (Dan Liu)

**Abstract:** The flotation separation of fluorite and calcite poses one of the most difficult problems in the mineral processing industry. In particular, the surface homogenization of fluorite and calcite worsens the result of fluorite flotation. In this paper, time of flight secondary ion mass spectrometry and principal component analysis are used to study the surface homogenization of fluorite and calcite during grinding and in solution using X-ray photoelectron spectroscopy, infrared spectroscopy, and solution chemical calculations. The results show that the surface composition of calcite converts to fluorite after mixed grinding and that the surface composition of fluorite also converts to calcite in clarified calcite solution.

**Keywords:** homogenization phenomena, surface composition, fluorite, calcite, mixed grinding

### 1. Introduction

Fluorite ( $\text{CaF}_2$ ) is presently the main mineral source of fluorine. The special properties of fluorine have led to the wide use of fluorite in traditional and emerging industries, such as metallurgy, chemicals, ceramics, optics, and new energy (Peng et al., 2014; Zhou et al., 2013). Calcite ( $\text{CaCO}_3$ ) is a common gangue mineral in fluorite ore. The separation of fluorite from gangue minerals is difficult owing to their similar surface properties and floatability (Gao, Bai, Sun, Cao, & Hu, 2015; Liu, Feng, Zhang, Chen, & Chen, 2016), and the homogenization of mineral surfaces in the coexisting system further increases the difficulty of fluorite selective flotation separation.

Previous studies have mainly focused on the selective collectors, inhibitors, and mechanism of fluorite and calcite separation during the flotation process. However, few studies and verifications have addressed their surface homogenization (Jiang et al., 2018; Tian et al., 2019; Zhang et al., 2017; Zhou et al., 2020; Zhu et al., 2018).

On the basis of the chemical theory of a flotation solution, Hu (1989) proposed that the following reactions occur between fluorite and calcite in solution:



Miller and Hiskey (1972) reported that  $\text{CO}_3^{2-}$  in the solution reacts with fluorite and generates calcite on its surface, which affects the former's electrochemical behavior, in a process that they termed the surface carbonization phenomenon of fluorite.

The above studies are limited to the possible mutual transformation of fluorite and calcite in solution. However, no systematic study has been conducted to investigate the transformation of fluorite and calcite during the mixed grinding process and its effect on the mineral surface composition. Previous results have shown that the mineral composition and grinding conditions strongly impact the

subsequent flotation process (Bruckard et al., 2011) and is therefore worthy of further detailed investigation.

This study verifies the transformation phenomenon of fluorite and calcite in coexisting solution and proposes that the surface compositions of these two minerals change to become more similar during dry grinding; namely, the surface homogenization of fluorite and calcite. This study provides a theoretical basis for controlling or eliminating this phenomenon by optimizing the grinding conditions and is therefore of great significance for improving the flotation effect of fluorite.

In this paper, the surface composition changes of fluorite and calcite during grinding were studied by time of flight secondary ion mass spectrometry (ToF-SIMS), and a principal component analysis (PCA) model was established to group and analyze the results. For comparison, the surface homogenization of fluorite in clarified calcite solution was studied by X-ray photoelectron spectroscopy (XPS), infrared spectroscopy, and solution chemical calculations.

## 2. Materials and methods

### 2.1. Materials

The X-ray diffraction (XRD) analyses of the fluorite and calcite minerals used in this study are shown in Fig. 1. The XRD patterns show that the samples can essentially be regarded as pure minerals. The minerals were ground with a three-head grinder (XPM- $\Phi$ 120  $\times$  3, China), screened between 44 and 74  $\mu$ m, and then sealed and stored.

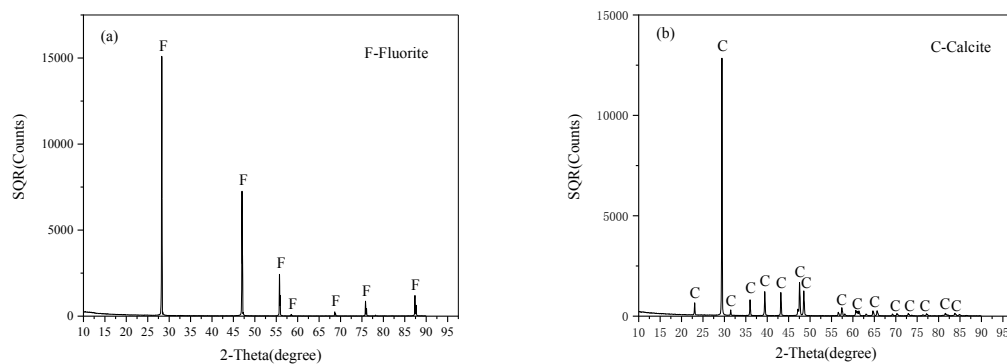


Fig. 1. XRD pattern of (a) pure fluorite and (b) pure calcite samples

### 2.2. Sample preparation

#### 2.2.1. Sample preparation in the grinding process

Fluorite (2 g), calcite (2 g), and mixed ore samples (1 g fluorite + 1 g calcite) of 44–74  $\mu$ m size fraction were ground with a three-head grinder. After grinding for 2 min 30 s, 2 mL of deionized water was used to rinse the samples into a filter funnel. The filtered samples were dried in air for 2 h and then immediately analyzed by ToF-SIMS. The agate mortar and grinding head were cleaned before each grinding with anhydrous alcohol and deionized water.

#### 2.2.2. Sample preparation of coexisting solution

Calcite (5 g) and deionized water (150 mL) were added to a beaker, stirred for 15 min, and then filtered to obtain a clarified calcite solution with a pH of 9.6. Fluorite (2 g) and the clarified calcite solution (100 mL) were then added to a beaker, stirred with a magnetic stirrer for 30 min, and rinsed into a filter funnel. After the filtered samples were dried in air for 2 h, these samples were used for XPS and infrared spectrum analyses.

### 2.3. ToF-SIMS analysis

Ground samples were used for ToF-SIMS analysis using a ToF-SIMS V (ION-TOF GmbH, Münster, Germany) with a 15-keV  $\text{Bi}_3^+$  primary ion beam pulse with stops after 112 s of analysis in sawtooth mode. A 256  $\times$  256 pixel density and less than 5  $\times$  5  $\mu$ m pixel size was used in a 500  $\times$  500  $\mu$ m region.

## 2.4. XPS analysis

Samples of the coexisting solution and pure calcite were used for the ToF-SIMS analysis. The multi-functional scanning imaging photoelectron spectroscopy (phi5000 versaprobe II) instrument was used for the XPS analysis. The instrument power was set to 50 W, the voltage was 15kV, the anode was an Al target, and the correction was C1s: 284.8 eV. MultiPak 9.3 software was used to fit the peaks to the XPS data to determine the relative concentrations of elements and analyze the binding energy.

## 2.5. Infrared spectrum analysis

Samples of the coexisting solution, pure calcite, and pure fluorite were analyzed using a Bruker alpha infrared spectrometer. The analytical range of the instrument was 400–4000  $\text{cm}^{-1}$ , the scanning time was 16 s, and the spectral resolution was 4  $\text{cm}^{-1}$ .

## 2.6. Solution chemistry calculations

The Visual MINTEQ (3.1 version) program was used to calculate the existence form and ion content in the coexisting solution of fluorite and calcite and the saturation index (SI) of the potential minerals in the system. The change of ion content and potential minerals in the coexisting solution with pH was drawn according to the Visual MINTEQ model data.

## 3. Results and discussion

### 3.1. ToF-SIMS imaging analysis

Fig. 2a shows a 100x magnified image of the ore samples of fluorite and calcite after mixing and separate grinding. The green square outlines a  $500 \times 500 \mu\text{m}$  analysis area with a pixel density of  $256 \times 256$  and lateral resolution of  $<5 \mu\text{m}$ . Figs. 2b–2d show images of  $\text{Ca}_2\text{F}_3^+$ ,  $\text{Ca}_2\text{O}_2^+$ , and an overlay of  $\text{Ca}_2\text{F}_3^+$  and  $\text{Ca}_2\text{O}_2^+$ , respectively, in which  $\text{Ca}_2\text{F}_3^+$  and  $\text{Ca}_2\text{O}_2^+$  are the representative ions produced by fluorite and calcite during grinding. In the ion images, bright colors represent the regions of higher ion intensity and dark colors represent the regions of lower ion intensity.

The results in Fig. 2 indicate that the ion distribution of  $\text{Ca}_2\text{F}_3^+$  and  $\text{Ca}_2\text{O}_2^+$  in the mixed ore sample with separate fluorite and calcite grinding shows an opposite trend. In particular, the region with high  $\text{Ca}_2\text{F}_3^+$  intensity has low  $\text{Ca}_2\text{O}_2^+$  intensity, whereas the region with low  $\text{Ca}_2\text{F}_3^+$  intensity has high  $\text{Ca}_2\text{O}_2^+$  intensity. The overlay image of  $\text{Ca}_2\text{F}_3^+$  and  $\text{Ca}_2\text{O}_2^+$  also shows that the two ions have a clear boundary, which can be easily distinguished by the red and green colors.

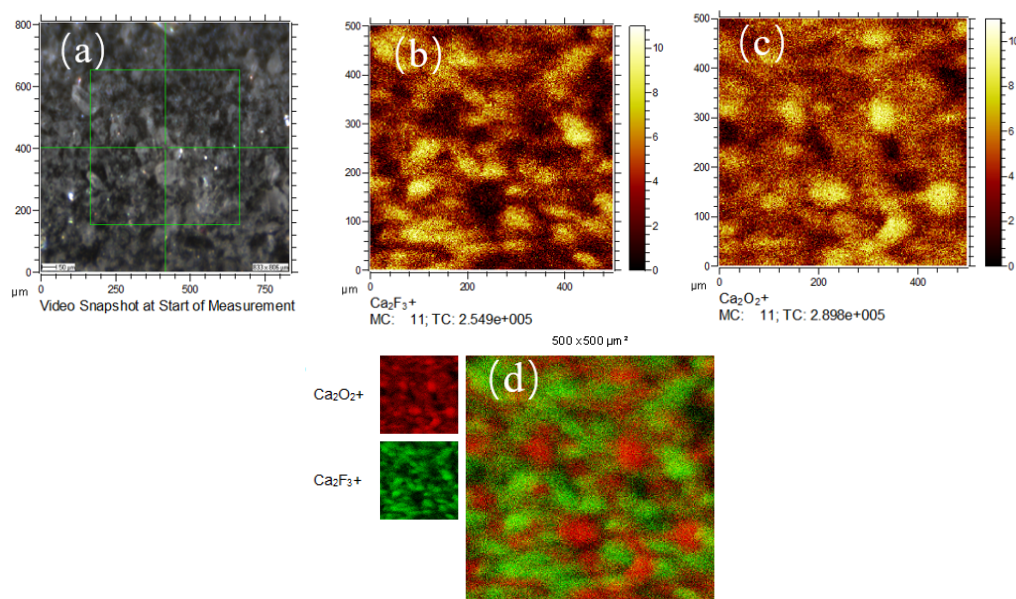


Fig. 2. (a) 100x digital image of the mixed ore sample after separate grinding. (b)–(d) Images of  $\text{Ca}_2\text{F}_3^+$ ,  $\text{Ca}_2\text{O}_2^+$ , and an overlay of  $\text{Ca}_2\text{F}_3^+$  and  $\text{Ca}_2\text{O}_2^+$ , respectively

Fig. 3 shows images of the fluorite and calcite sample after mixed grinding. Compared with the images of the mixed ore sample in Fig. 2, it can be observed that the ion distribution of  $\text{Ca}_2\text{F}_3^+$  and  $\text{Ca}_2\text{O}_2^+$  becomes more similar (e.g., some regions with high  $\text{Ca}_2\text{F}_3^+$  intensity also have high  $\text{Ca}_2\text{O}_2^+$  intensity). The overlay image of  $\text{Ca}_2\text{F}_3^+$  and  $\text{Ca}_2\text{O}_2^+$  in Fig. 3 also shows that the boundary between the two ions is no longer as clear as that in Fig. 2d; some red areas are covered with green and the boundary is blurred. The results show that ion migration occurred during the mixed grinding process and some  $\text{Ca}_2\text{F}_3^+$  ions migrated from the fluorite surface to the calcite surface.

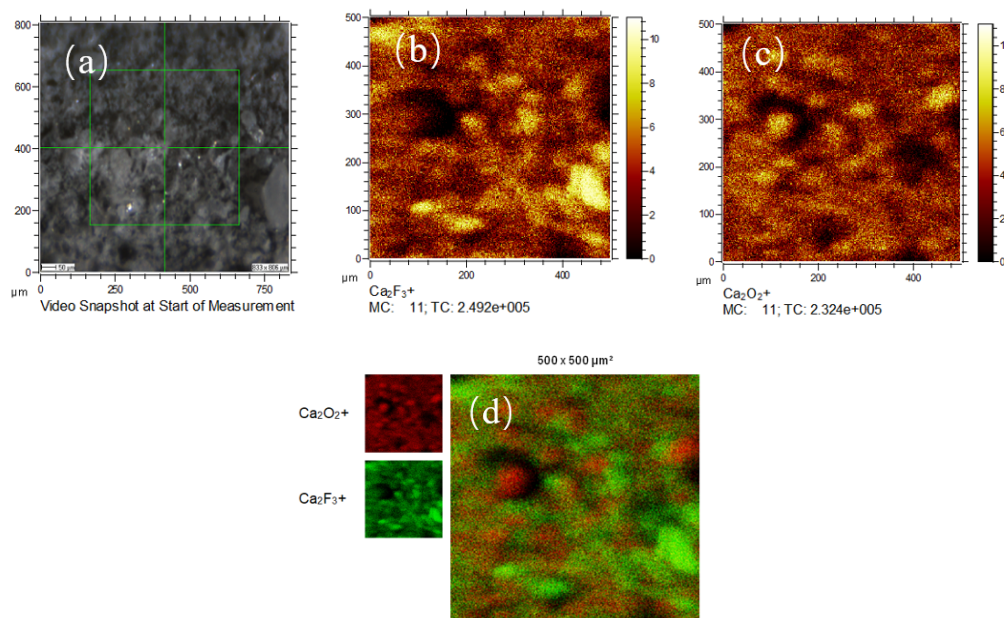


Fig. 3. (a) 100x digital image of the mixed ore sample after mixed grinding. (b)–(d) Images of  $\text{Ca}_2\text{F}_3^+$ ,  $\text{Ca}_2\text{O}_2^+$ , and an overlay of  $\text{Ca}_2\text{F}_3^+$  and  $\text{Ca}_2\text{O}_2^+$ , respectively

### 3.2. ToF-SIMS statistical analysis

The ToF-SIMS ion imaging analysis qualitatively indicates that a portion of  $\text{Ca}_2\text{F}_3^+$  migrated from the fluorite surface to the calcite surface during the mixed grinding process, but the effect of this phenomenon on the calcite surface composition remains unknown. To explore the changes of surface composition of the mixed mineral samples, SurfaceLab 6.8 software was used to overlay the ion images, normalize the intensity of each positive ion peak with the total ion intensity statistics of its spectrum, and draw a column chart after statistical analysis, as shown in Fig. 4. The dark red, light red, orange, and light yellow bars represent the fluorite in the mixed ore sample after separate grinding, fluorite in the ore sample after mixed grinding, calcite in the mixed ore sample after separate grinding, and calcite in the ore sample after mixed grinding, respectively.

The  $\text{CaF}^+$  and  $\text{Ca}_2\text{F}_3^+$  intensities on the calcite surface clearly increase after mixed grinding, whereas the  $\text{Ca}_2\text{O}_2^+$  and  $\text{Ca}_2\text{O}_3^+$  intensities decrease. The intensity of the four ions on the surface of fluorite also changed slightly after mixed grinding.  $\text{CaF}^+$  and  $\text{Ca}_2\text{F}_3^+$  are representative ions of fluorite and  $\text{Ca}_2\text{O}_2^+$  and  $\text{Ca}_2\text{O}_3^+$  are representative ions of calcite. Combined with the ToF-SIMS imaging analysis, it can be concluded that during mixed grinding,  $\text{CaF}^+$  and  $\text{Ca}_2\text{F}_3^+$  generated on the fluorite surface migrate and adsorb on the calcite surface, which changes the calcite surface composition and the fluorite surface also adsorbs a small amount of ions generated on the calcite surface.

### 3.3. PCA model analysis

PCA is a data dimension reduction algorithm that is widely used to process ToF-SIMS data. PCA can reduce the dimension of complex ToF-SIMS data and simplify the spectra for analysis (Deng et al., 2013; Berman et al., 2009; Park et al., 2010; Tyler et al., 2007). The PCA model based on the ToF-SIMS data of the separate and mixed ground samples is shown in Fig. 5. The blue circle represents the calcite after

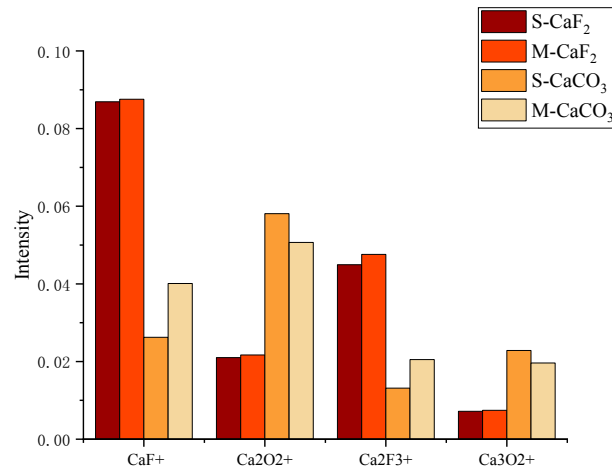


Fig. 4. Normalized statistical analysis of ionic strength

mixed grinding, the yellow circle represents the calcite after separate grinding, the green circle represents the fluorite after mixed grinding, and the red circle represents the fluorite after separate grinding. The coordinate axes in the figure indicate the relative distance. Smaller relative distances are associated with more similar surface compositions.

The figure shows that the surface composition of calcite after mixed grinding strongly differs from that after separated grinding. Moreover, the surface composition of calcite after mixed grinding is closer to fluorite on the right side of the figure compared with calcite after separate grinding. The fluorite position after mixed grinding in the coordinate system has also changed. By combining the ToF-SIMS imaging, statistical analyses, and PCA model analysis, the results show that the surface composition of calcite is closer to fluorite after mixed grinding and the surface composition of fluorite also changes.

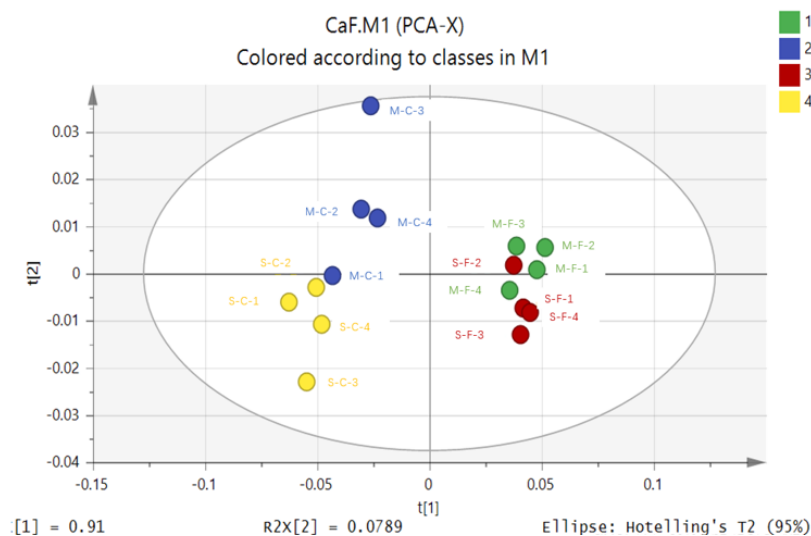


Fig. 5. PCA model based on ToF-Sims spectral data

### 3.4. XPS spectral analysis

To study the surface homogenization of fluorite and calcite in coexisting solution, the pure mineral samples of fluorite and fluorite samples after reaction in the clarified calcite solution with a pH of 9.6 were analyzed by XPS. The XPS spectrum of Ca<sub>2</sub>p in the samples before and after the reaction was determined by peaking fitting and the results are shown in Fig. 6.

The binding energy of the Ca<sub>2</sub>p peak shifted from 348.09 to 347.00 eV after the reaction. Compared with the standard spectra (Moulder, 1992), the binding energy of Ca<sub>2</sub>p represents CaF<sub>2</sub> at 348.09 eV and CaCO<sub>3</sub> at 347.00 eV, which indicates that the sample surface compositions were converted from fluorite to calcite after the reaction.

Fig. 7 shows the semi-quantitative analysis results of the surface compositions of the samples before and after the reaction, in which the yellow bars represent the pure fluorite samples and the green bars represent the fluorite samples after reaction in the clarified calcite solution.

The relative contents of C and O atoms in the sample increased after the reaction, whereas the relative content of F atoms decreased. This result is consistent with the conclusions of Miller and Hiskey (1972).

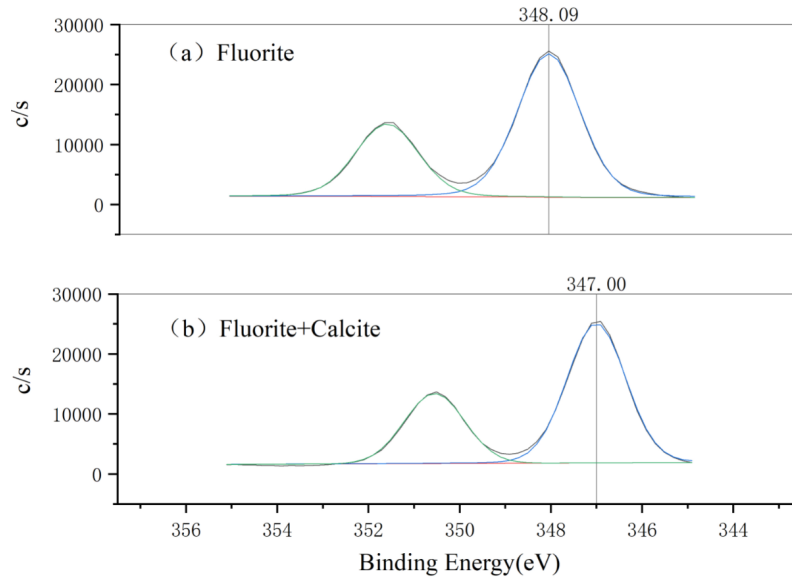


Fig. 6. Ca<sub>2p</sub> XPS spectra of (a) pure fluorite and (b) fluorite reacted in clarified calcite solution

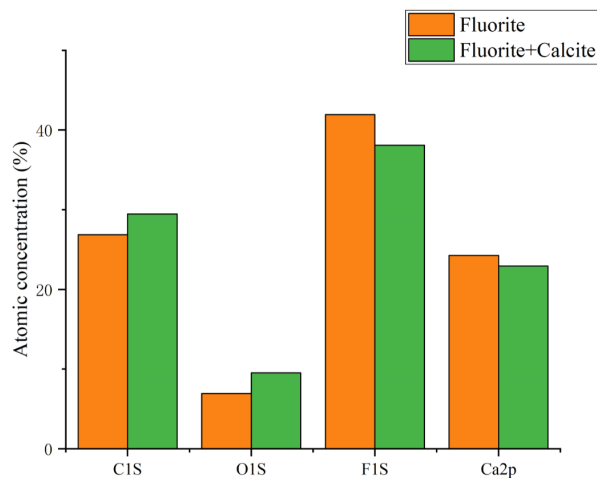


Fig. 7. Relative atomic content of the fluorite surface before and after reaction

### 3.5. Infrared spectrum analysis

The infrared spectrum analysis results of the pure fluorite samples, pure calcite samples, and fluorite samples after reaction are shown in Figs. 8a–8c, respectively. The absorption valley of  $\text{CO}_3^{2-}$  is observed between wave numbers 1530 and 1320  $\text{cm}^{-1}$  in Fig. 8b (Nakamoto & Huang, 1986) and to a lesser extent in Fig. 8c, but not in Fig. 8a. This indicates that fluorite is converted to calcite after reaction in the calcite clear solution, which is consistent with the XPS results.

### 3.6. Solution chemistry calculations

It is necessary to use solution chemistry calculations to calculate the morphology, solubility balance, and adsorption of ions in aqueous solutions (Gerson et al., 2012; Liu et al., 2020; Markovski et al., 2014). The effect of pH on the form of carbonate ions in the coexisting solution of fluorite and calcite is shown in Fig. 9a.  $\text{H}_2\text{CO}_3(\text{aq})$  dominates for  $\text{pH} < 6.3$ . When  $\text{pH} > 6.3$ ,  $\text{HCO}_3^-$  and  $\text{CO}_3^{2-}$  are in turn dominant.

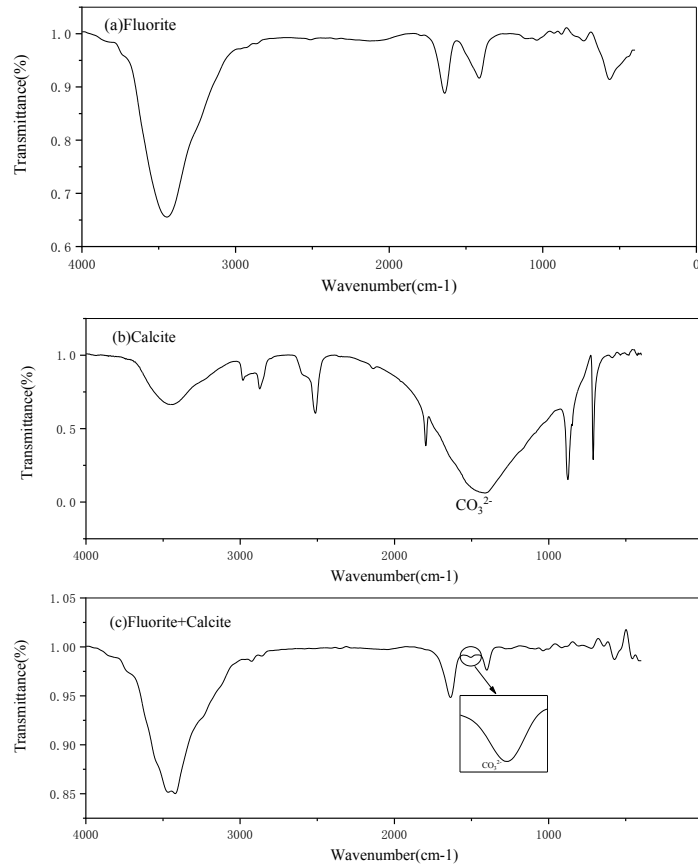


Fig. 8. Infrared spectra of (a) pure fluorite, (b) pure calcite, and (c) fluorite samples reacted in clarified calcite solution

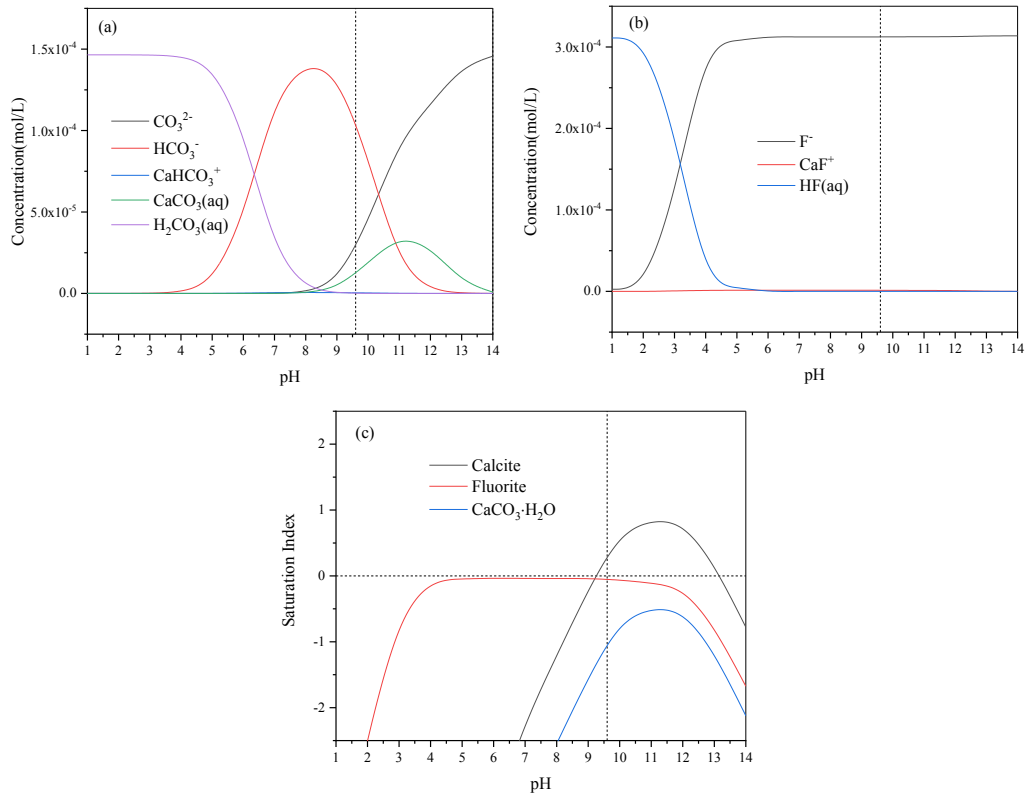


Fig. 9. Effects of pH on (a) carbonate ion speciation in the coexisting solution and (b) fluoride ion speciation in the coexisting solution. (c) SIs of the potential minerals in the coexisting solution

When pH = 9.6, the content of the components in the solution follows  $\text{HCO}_3^- > \text{CO}_3^{2-} > \text{CaHCO}_3^- > \text{H}_2\text{CO}_3(\text{aq})$ , and the main chemical reactions of the ions in the solution are as follows.



At this pH value, the  $\text{CO}_3^{2-}$  content in the solution is high, which is expected to combine with  $\text{Ca}^{2+}$  dissociated from fluorite to form  $\text{CaCO}_3$  and adsorbed on the surface of minerals.

$\text{HF}(\text{aq})$  dominates when  $\text{pH} < 3.2$ ,  $\text{F}^-$  dominates when  $\text{pH} > 3.2$ , and the  $\text{CaF}^+$  content is consistently low (Fig. 9b). When  $\text{pH} = 9.6$ , the main component in the solution is  $\text{F}^-$ , and the main chemical reaction of the ions in the solution is as follows.



At this pH value, fluorite dissociates into a large amount of  $\text{Ca}^{2+}$  which can combine with  $\text{CO}_3^{2-}$  to form  $\text{CaCO}_3$ .

Fig. 9c shows the SI values of the potential minerals in solution as a function of pH. When the  $\text{SI} > 0$ , a solid phase may form (Arocena & Glowa, 2000). For  $\text{pH} = 9.6$ , the SIs of fluorite, calcite, and  $\text{CaCO}_3 \cdot \text{H}_2\text{O}$  are  $-0.052$ ,  $0.275$ , and  $-1.060$ , respectively, which means that  $\text{CaCO}_3$  precipitation is easier to form under this pH condition. The solution chemistry calculations verify the detection and analysis results of the XPS and infrared spectroscopy.

#### 4. Conclusions

Mineral surface homogenization is one of the most important factors that affects the flotation separation of fluorite and calcite. However, the transformation trend of fluorite and calcite in the mixed grinding process is inconsistent with that in the coexisting solution.

Through the analysis of the ToF-SIMS data and PCA model, the results show that the ions generated on the surface of fluorite will migrate to the surface of calcite, which makes the surface composition of calcite closer to that of fluorite, while the ions generated on the surface of calcite have poor adsorption capacity on the fluorite surface.

The XPS, infrared spectroscopy analysis, and solution chemistry calculation results show that the surface composition of fluorite converts to calcite under the action of  $\text{CO}_3^{2-}$  in weakly alkaline clarified calcite solution.

The discovery and verification of the surface homogenization of fluorite and calcite in this study provides a new perspective on why fluorite and calcite are difficult to separate. However, further study is required to develop an effective method to control and eliminate surface homogenization to improve the selective flotation separation effect of fluorite.

#### Acknowledgments

We are grateful to the Analysis and Testing Centre in Kunming University of Science and Technology for technical support.

#### References

- AROCENA, J. M., GLOWA, K. R., 2000. *Mineral weathering in ectomycorrhizosphere of subalpine fir (Abies lasiocarpa (Hook.) Nutt.) as revealed by soil solution composition*. Forest Ecology & Management, 133(1-2), 61-70.
- BERMAN, E.S.F., WU, L., FORTSON, S.L., KULP, K.S., NELSON, D.O., WU, K.J., 2009. *Chemometric and statistical analyses of ToF-SIMS spectra of increasingly complex biological samples*. Surface & Interface Analysis, 41, 97-104.
- BRUCKARD, W. J., SPARROW, G. J., WOODCOCK, J. T., 2011. *A review of the effects of the grinding environment on the flotation of copper sulphides*. International Journal of Mineral Processing, 93(1-2), 1-13.
- DENG, J. S., WEN, S. M., WU, D. D., LIU, J., ZHANG, X. L., SHEN, H. Y., 2013. *Existence and release of fluid inclusions in bornite and its associated quartz and calcite*. International Journal of Minerals Metallurgy and Materials, 20(009), 815-822.
- GAO, Z., BAI, D., SUN, W., CAO, X., HU, Y., 2015. *Selective flotation of scheelite from calcite and fluorite using a collector mixture*. Minerals Engineering, 72, 23-26.

- GERSON, A. R., SMART, R. S. C., LI, J., KAWASHIMA, N., WEEDON, D., TRIFFETT, B., BRADSHAW, D., 2012. *Diagnosis of the surface chemical influences on flotation performance: Copper sulfides and molybdenite*. International Journal of Mineral Processing, 106-109(none), 16-30.
- HU, Y. H. (1989). *Study on Solution Chemistry Calculation and Graphic Method and Flotation Behavior of Salt Minerals*. Central South University of Technology,
- JIANG, W., GAO, Z., KHOSO, S. A., GAO, J., SUN, W., PU, W., HU, Y., 2018. *Selective adsorption of benzhydroxamic acid on fluorite rendering selective separation of fluorite/calcite*. Applied Surface Science, 435(MAR.30), 752-758.
- LIU, C., FENG, Q., ZHANG, G., CHEN, W., CHEN, Y., 2016. *Effect of depressants in the selective flotation of scheelite and calcite using oxidized paraffin soap as collector*. International Journal of Mineral Processing, 157, 210-215.
- LIU, C., ZHOU, M., XIA, L., FU, W., YANG, S., 2020. *The utilization of citric acid as a depressant for the flotation separation of barite from fluorite*. Minerals Engineering, 156, 106491.
- MARKOVSKI, J.S., MARKOVIĆ, D.D., ĐOKIĆ, V.R., MITRIĆ, M., MARINKOVIĆ, A.D., 2014. *Arsenate adsorption on waste eggshell modified by goethite,  $\alpha$ -MnO<sub>2</sub> and goethite/ $\alpha$ -MnO<sub>2</sub>*. Chemical Engineering Journal, 237, 430-442.
- MILLER, J.D., HISKEY, J.B., 1972. *Electrokinetic behavior of fluorite as influenced by surface carbonation*. Journal of Colloid & Interface Science, 41(3), 567-573.
- MOULDER, J. F., 1992. *Handbook of X-ray Photoelectron Spectroscopy*, Physical Electronics Division, Perkin-Elmer Corporation, pp. 261
- NAKAMOTO, K., HUANG, D.R., 1986. *Infrared and Raman spectra of inorganic and coordination compounds*. Chemical Industry Press.
- PARK, J. W., MIN, H., KIM, Y. P., SHON, H. K., KIM, J., MOON, D. W., LEE, T. G., 2010. *Multivariate analysis of ToF-SIMS data for biological applications*. Surface & Interface Analysis, 41(8), 694-703.
- TIAN, J., XU, L., SUN, W., ZENG, X., FANG, S., HAN, H., HONG, K., HU, Y., 2019. *Use of Al<sub>2</sub>(SO<sub>4</sub>)<sub>3</sub> and acidified water glass as mixture depressants in flotation separation of fluorite from calcite and celestite*. Minerals Engineering, 137, 160-170.
- TYLER, B. J., RAYAL, G., CASTNER, D. G., 2007. *Multivariate analysis strategies for processing ToF-SIMS images of biomaterials*. Biomaterials, 28(15), 2412-2423.
- PENG, W.J., ZHANG, L.Y., BAI, L.L., QIU, Y.S., 2014. *Flotation research of a fluorite ore*. Appl. Mech. Mater., 539, 781-784.
- ZHANG, C., WEI, S., HU, Y., TANG, H., GAO, J., YIN, Z., GUAN, Q., 2017. *Selective adsorption of tannic acid on calcite and implications for separation of fluorite minerals*. Journal of colloid and interface science, 512, 55.
- ZHOU, H., ZHANG, Y., TANG, X., CAO, Y., LUO, X., 2020. *Flotation separation of fluorite from calcite by using psyllium seed gum as depressant*. Minerals Engineering, 159, 106514.
- ZHOU, W., MORENO, J., TORRES, R., VALLE, H., SONG, S., 2013. *Flotation of fluorite from ores by using acidized water glass as depressant*. Minerals Engineering, 45, 142-145.
- ZHU, H., QIN, W., CHEN, C., CHAI, L., JIAO, F., JIA, W., 2018. *Flotation separation of fluorite from calcite using polyaspartate as depressant*. Minerals Engineering, 120, 80-86.